A New Fluorinated Polyurethane: Polymerization, Characterization, and Mechanical Properties

Tai Ho*,[1]

Department of Chemistry, George Mason University, 4400 University Drive, Fairfax, Virginia 22030-4444

Kenneth J. Wynne*

Materials Chemistry Branch, Naval Research Laboratory, Washington, D.C. 20375-5000, and Chemistry Division, Office of Naval Research, 800 North Quincy Street, Arlington, Virginia 22217-5000

Received October 21, 1991; Revised Manuscript Received March 5, 1992

ABSTRACT: A fluorinated polyurethane based on the ethylene–fluoroalkyl–ethylene diol 3-(trifluoromethyl)-3,4,4,5,5,6,6,7,7,8,8-undecafluoro-1,10-decanediol, $HO(CH_2)_2(CF_2)_4(CF_2CFCF_3)(CH_2)_2OH$ (including 5% 4-trifluoromethyl isomer), and 1,6-hexamethylene diisocyanate, $OCN(CH_2)_6NCO$, was prepared. The kinetics of polymerization was studied using Fourier transform infrared spectroscopy. The resulting polyurethane was characterized by viscometry, differential scanning calorimetry (DSC), and gel permeation chromatography. Correlations among the glass transition temperature, intrinsic viscosity, and molecular weight were established. Interestingly, multiple exotherms appeared in the DSC data, the areas and positions of which were time-dependent. The appearance of ordered domains in the solid state correlated with the decreased ratio of the "free" to "bound" C=O stretching frequencies in the infrared spectra. The effect of this apparent crystallization on mechanical properties was evaluated via stress–strain and dynamic mechanical testing.

Introduction

The incorporation of toxicants such as copper and tributyltin oxide[2,3] in coatings has been the standard method for preventing settlement of organisms on ship hulls and other structures exposed to the marine environment. Many approaches have been used to gain control over toxicant release rate so as to prolong coating life and minimize environmental impact.[4,5] Problems with toxicant release include adverse environmental effects from leached toxicants, even at sub-microgram/liter levels,[6] and disposal of large quantities of toxic waste when coatings are removed during refurbishing.

A potential alternative to toxicant release is a surface to which fouling organisms adhere with difficulty. Incorporated into a coating, such surfaces would be intrinsically fouling resistant,[7] would effect facile fouling release, and would be environmentally benign. Ideally, in the event of organism settlement, removal would be effected by flowing water as, for example, that generated by a ship under way or by pumped water in a heat exchanger. The concept of fouling release coatings has been demonstrated in the development of coatings with resin matrices compatible with Teflon fillers.[7] It is important, however, to extend this progress to answer questions concerning the connection of fundamental polymer properties with the tendency of adhesion of fouling organisms.

It is postulated that adhesion of organisms to a polymer surface is dependent on more than just surface composition which controls parameters such as hydrophobicity, surface energy, and acid–base interactions. We believe that the surface physical state (glass, crystal, liquid, rubber) is also an important parameter. Overall, the features which are desired for prevention of adhesion of marine organisms may be related to those features which incorporate antithrombogenic activity in polymers.[8]

The availability of a new family of fluorinated diols[9] of the formula $HOC_2H_4(CF_2CF_3CF)_x(CF_2)_4(CF_2CFCF_3)_yC_2H_4OH$ led to interest in the incorporation of these monomers into polymers which might have interesting surface properties. This paper concerns the polyurethane derived from one of the members of this family of diols, $HO(CH_2)_2(CF_2)_4(CF_2CFCF_3)(CH_2)_2OH$ (1), and hexamethylene diisocyanate (HDI). The interesting solid-state properties displayed by this polymer resulted in the separate study reported herein. Work on related polymers containing diols with more than one $-(CF_2CFCF_3)-$ group per diol will be reported separately. This work is related to prior efforts on the incorporation of fluorinated hydroxyl-terminated polyethers into polyurethanes.[10]

Experimental Section

Materials. The ethylene–fluoroalkyl–ethylene diol 1, also referred to as "C_7-diol", as it contains seven fluorocarbon carbon atoms, was provided by K. Baum, Fluorochem, Inc., Azusa, CA. Because of the nature of the free-radical addition of perfluoropropylene shown in Scheme I, 1 is obtained as a mixture of isomers

$$HO(CH_2)_2(CF_2)_4(CF_2CFCF_3)(CH_2)_2OH \quad \sim 95\%$$

$$HO(CH_2)_2(CF_2)_4(\underset{1}{CFCF_3CF_2})(CH_2)_2OH \quad \sim 5\%$$

as shown below.[9] HDI was MONDUR HX from Mobay Chemical. C_7-diol was used as received; HDI was distilled under vacuum before use.

Polymerization. A typical reaction was carried out as described below. A portion of C_7-diol (ca. 3 g) was degassed and mixed with an equimolar portion of HDI at 55 °C under nitrogen. After the appearance of a clear homogeneous solution, the mixture was heated or cooled to a chosen reaction temperature and a minute amount of dibutyltin dilaurate (less than 0.05% by weight) was added as catalyst. The reaction was allowed to proceed at that temperature for 4 h and then at ambient temperature overnight. Fourier transform infrared (FTIR) spectroscopy was used to monitor the progress of the reaction. At the end of the reaction, the product was heated to ~90 °C, and the product was scraped out of the reaction vessel onto a Teflon surface. After cooling to ambient temperature, the solid polymer was easily separated and isolated. The resulting polyurethane, polymer 2, was characterized with viscometry, differential scanning calorimetry (DSC), and gel permeation chromatography (GPC). Mechanical properties of this material were also evaluated.

IR Spectroscopy. FTIR spectra were collected using a Perkin-Elmer 1800 FTIR spectrometer. To study the course of the reaction, the components were mixed with catalyst and heated as described above. This mixture was sampled at regular intervals to assess the progress of the polymerization reaction. Samples,

0024-9297/92/2225-3521$03.00/0

being viscous liquid, were coated directly onto KBr plates for measurement.

NMR Spectroscopy. Proton NMR spectra were recorded on a Bruker MSL-300 FTNMR spectrometer with the sweep frequency at 300 MHz and the temperature at 25 °C. Samples were dissolved in deuterated chloroform with tetramethylsilane (TMS) as an internal reference. Peaks for the C_7-diol (assigned in Figure 3A) were at (δ vs TMS) 1.76, 2.44 (br m, ca. 12 peaks), and 3.98 (5-peak m). For HDI[11] (Figure 3B): multiplets at 1.39 and 1.62 and a triplet at 3.30 (6.6 Hz). Polymer **2** displayed six peaks (Figure 3C): 1.33, 1.49, 2.46 (br m), 3.15 (t, 6 Hz), 4.32 (m), and 4.91.

Viscometry. The intrinsic viscosity was determined with a Cannon-Fenske type (No. 50) viscometer immersed in a water bath controlled at 25 °C. Solutions in tetrahydrofuran (THF) were used.

Differential Scanning Calorimetry (DSC). The glass transition and melting behavior of the polymer were detected with a Perkin-Elmer DSC 7. The scan rate was 10 °C/min. Melting data were collected in the first heating and cooling cycle, and the glass transition temperature (T_g) was determined in the second cycle to ensure the sample was amorphous.

Gel Permeation Chromatography (GPC). The molecular weight was determined by GPC. The equipment consisted of a Beckman Model 100A pump and an Altex μ-spherogel column (size 10^4 Å). The polymer contents in the effluent of the column were detected with a differential refractometer (Waters series R-400), and the average molecular weights were determined using polystyrene standards as references.

Mechanical Tests. Stress–strain tests were performed in an Instron Universal Testing Instrument (Model 4206). Standard type V specimens as specified in ASTM Standards, Method D-638, were used. Dynamic mechanical properties were evaluated with a Rheovibron dynamic viscoelastometer. Strips 5 mm wide and 10–15 mm long were used for this measurement.

Results and Discussion

The fluorinated diol 1 which we utilized[12] is prepared as shown in Scheme I. A mixture of fluorinated diols with

Scheme I

$$I(CF_2)_4I + CF_3CF{=}CF_2 \rightarrow I(CF_3CFCF_2)_x(CF_2)_4(CF_3CFCF_2)_yI$$

$$I(CF_3CFCF_2)_x(CF_2)_4(CF_3CFCF_2)_yI + C_2H_4 \rightarrow IC_2H_4(CF_3CFCF_2)_x(CF_2)_4(CF_3CFCF_2)_yC_2H_4I$$

$$IC_2H_4(CF_3CFCF_2)_x(CF_2)_4(CF_3CFCF_2)_yC_2H_4I + H_2SO_4{\cdot}SO_3 \rightarrow HOC_2H_4(CF_3CFCF_2)_x(CF_2)_4(CF_3CFCF_2)_yC_2H_4OH$$

$x = 0, 1,$ and 2 and $y = 0, 1,$ and 2 is formed in this manner. Diol 1 was isolated by fractional distillation and reacted with HDI to give polyurethane **2** according to Scheme II. Polymer **2** is clear and tough, readily forming films by

Scheme II

$$HOC_2H_4(CF_2)_4(CF_3CFCF_2)C_2H_4OH + OCNRNCO \rightarrow [OC_2H_4(CF_2)_4(CF_3CFCF_2)C_2H_4OC(O)NHRNHC(O)]_n$$

2

$$R = -(CH_2)_6-$$

solvent casting (tetrahydrofuran) or by melt pressing. Over the course of time, the polymer remains clear but slowly embrittles. Melt cast films used for preliminary evaluation of fouling release were quite brittle after a year. These observations led to a study of the time evolution of physical and mechanical properties described below.

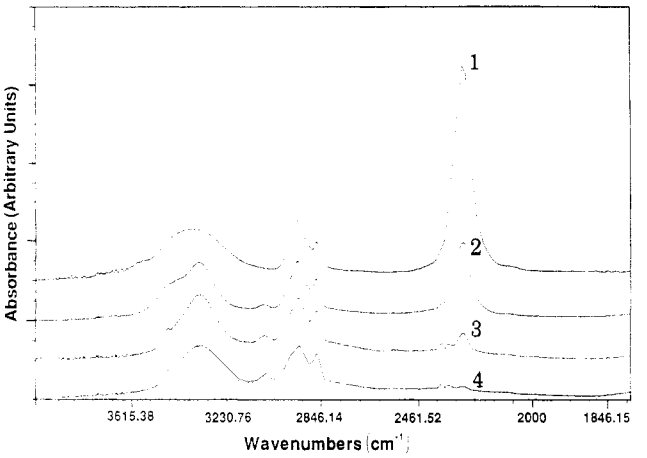

Figure 1. FTIR spectra of the reaction mixture during a typical polymerization reaction between C_7-diol and HDI: (1) starting mixture; (2) after 30 min at 58 °C; (3) after 1 h at 58 °C; (4) after 2 h at 58 °C.

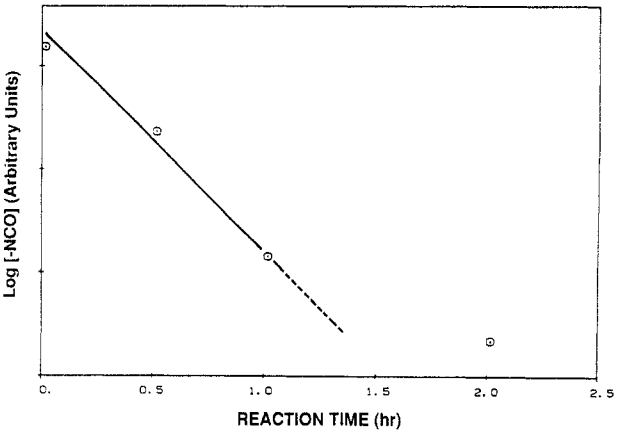

Figure 2. Concentration of the isocyanate group as a function of time during the first 2 h of a polymerization reaction between C_7-diol and HDI at 58 °C. The straight line is drawn to guide the eye.

Polymerization Reaction. The polymerization reaction was carried out at temperatures between 50 and 70 °C. At temperatures below 45 °C, the comonomers are only partially miscible and an equimolar mixture is not homogeneous. At temperatures higher than 70 °C, the reaction proceeds extremely fast, precluding uniform distribution of the catalyst.

Infrared spectra of the reaction mixture during a typical polymerization run are shown in Figure 1. The isocyanate absorption band centered at 2275 cm^{-1} was monitored to determine the extent of the reaction. As absorbance is concentration dependent and the concentrations of samples were not uniform, the data shown are normalized with respect to an arbitrary sample. In Figure 2, the concentration of the isocyanate group is plotted as a function of time. The data suggest a first-order reaction at the initial stage, but the apparent rate of reaction decreases significantly during the second hour. Since there is no large disparity between the reactivities of two isocyanate groups separated by an aliphatic chain,[13] the decrease in the reaction rate is likely due to the swift buildup of viscosity concurrent with polymerization. The rate constant, k, during the first hour of reaction at 58 °C was 6.51×10^{-4} s^{-1}.

In order to determine the activation energy, the rate constant at room temperature was determined. A small quantity of the reaction mixture (58 °C) was withdrawn 30 min after mixing and coated onto a KBr window. The specimen was then kept at 22 °C and the extent of the reaction monitored by FTIR spectroscopy. The sample

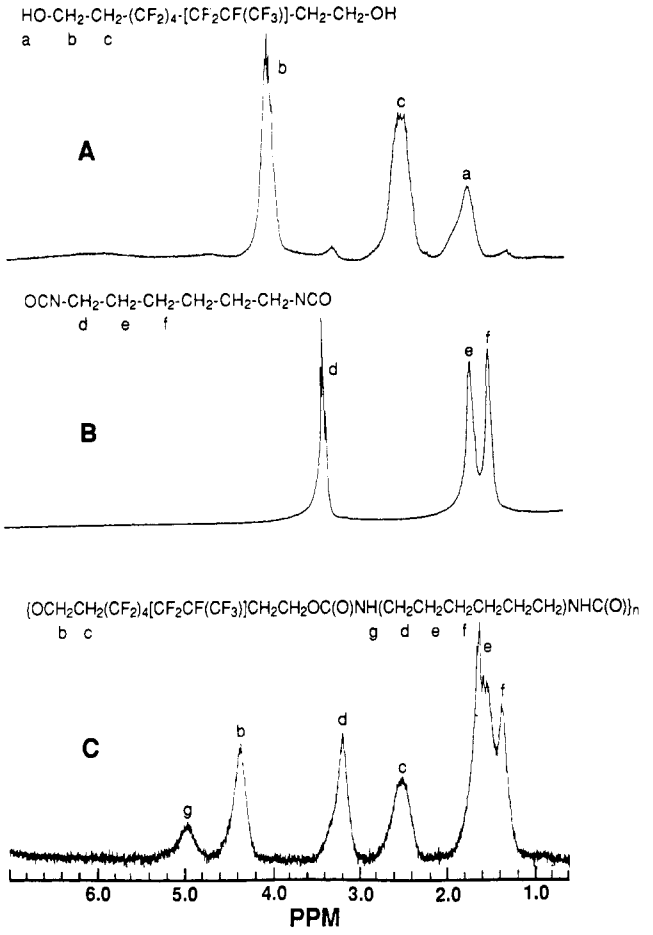

Figure 3. Proton NMR spectra for C_7-diol (A), HDI (B), and the resulting polymer (C).

remained optically clear throughout the measurement. The rate constant at room temperature (22 °C) was 0.41×10^{-4} s^{-1}, and the activation energy was 14.1 kcal mol^{-1}. These data may be compared with that obtained by Wong and Frisch for three aliphatic diisocyanates: *trans*-cyclohexane 1,4-diisocyanate (CHDI), isophorone diisocyanate (IPDI), and 4,4′-methylenebis(cyclohexyl) diisocyanate (HMDI).[14] In a model reaction with *n*-butanol (in toluene, 50 °C, dibutyltin dilaurate catalyst), a second-order reaction was found up to 50% conversion with rate constants of 1.40, 0.73, and 0.64 L mol^{-1} min^{-1} for CHDI, IPDI, and HMDI, respectively. The activation energy for CHDI was determined to be 17.78 kcal mol^{-1}.

The initial rate constant obtained in the present study in the absence of solvent was 6.51×10^{-4} s^{-1}. This implies a half-time at 17.7 min, which is comparable to Wong and Frisch's data (11.9–26.0 min). The activation energy for the reaction of 1 with HDI is similar to that reported by Wong and Frisch for CHDI with butanol.

Nuclear Magnetic Resonance Spectra. Proton NMR spectra for the monomers and polymer 2 are shown in Figure 3. With the formation of 2, the OH peak in the diol monomer at 1.76 ppm disappears and is replaced by a new peak at 4.91 ppm assigned to NH. Peaks due to the methylene groups adjacent to oxygen in the diol moved downfield by about 0.3 ppm, while methylene protons adjacent to nitrogen in the diisocyanate shifted upfield by ca. 0.15 ppm.

Molecular Weight, Intrinsic Viscosity, and Glass Transition Temperature. Eight batches of this fluorinated polyurethane were prepared. The number-average molecular weight, M_n, weight-average molecular weight, M_w, intrinsic viscosity, $[\eta]$, and glass transition temperature, T_g, for each batch were determined. These values

Table I
Molecular Weights, Glass Transition Temperatures, and Intrinsic Viscosities for a Series of Polyurethanes Derived from C_7-Diol and HDI[a]

sample	$M_n \times 10^{-3}$	$M_w \times 10^{-3}$	M_w/M_n	T_g (°C)	$[\eta]$ (dL/g)
1	12.5	19.2	1.5	11.7	0.16
2	14.1	26.7	1.9	11.7	0.16
3	18.2	33.5	1.8	15.5	0.23
4	27.6	51.2	1.9	16.0	0.28
5	28.0	65.5	2.3	17.4	0.37
6	33.1	80.3	2.4	17.7	0.38
7	38.7	70.5	1.8	18.2	0.35
8	59.4	222.0	3.7	19.7	0.60

[a] Molecular weights were obtained from GPC data, T_g by DSC, and intrinsic viscosity in tetrahydrofuran at 25 °C.

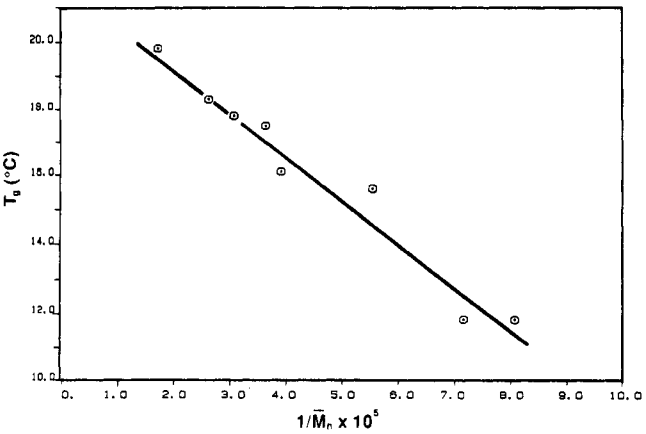

Figure 4. Glass transition temperature as a function of molecular weight for polyurethanes based on C_7-diol and HDI. The solid line is the best-fit line through the data points.

are listed in Table I. Typically, the number-average molecular weight is about 30 000 and the polydispersity (M_w/M_n) 2.0.

The glass transition temperature increases with increasing molecular weight and varies from 11.7 to 19.7 °C. In Figure 4, T_g of the polyurethane is plotted as a function of the reciprocal of its number-average molecular weight. A linear relationship of the Flory–Fox type has been found:

$$T_g\,(°C) = 21.7 - 1.29 \times 10^5/M_n \quad (1)$$

The intrinsic viscosity, in tetrahydrofuran at 25 °C, also increases with increasing molecular weight. The molecular weight (MW) of a monodisperse polymer is related to its intrinsic viscosity ($[\eta]$) through the Mark–Houwink–Sakurada equation

$$[\eta] = k_m(\mathrm{MW})^a \quad (2)$$

For polydisperse systems, eq 2 becomes

$$[\eta] = k_m(M_v)^a \quad (3)$$

where M_v is the viscosity-average molecular weight. M_v is a function of the mole fraction distribution function, $F(\mathrm{MW})$, of the system and the parameter a:[15]

$$M_v = f[F(\mathrm{MW}),a] \quad (4)$$

The mole fraction distribution function in turn can be derived from a GPC chromatogram.[16] By applying eqs 3 and 4 to all the batches prepared and solving the resulting simultaneous equations, we obtained an optimum value for a at 0.624. A plot of $[\eta]$ as a function of M_v is shown in Figure 5. Unlike M_w and M_n, M_v can be derived from a GPC chromatogram only through a tedious calculation; therefore, it is of interest to know how M_v compares to the other more readily obtainable quantities. When M_w was

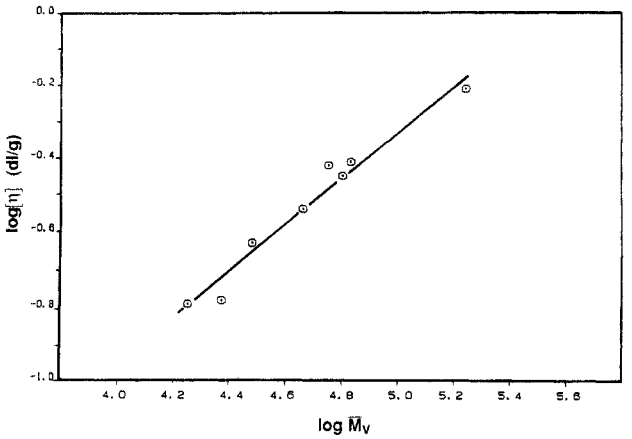

Figure 5. Intrinsic viscosity as a function of molecular weight for polyurethanes based on C_7-diol and HDI. The solid line is the best-fit line through the data points.

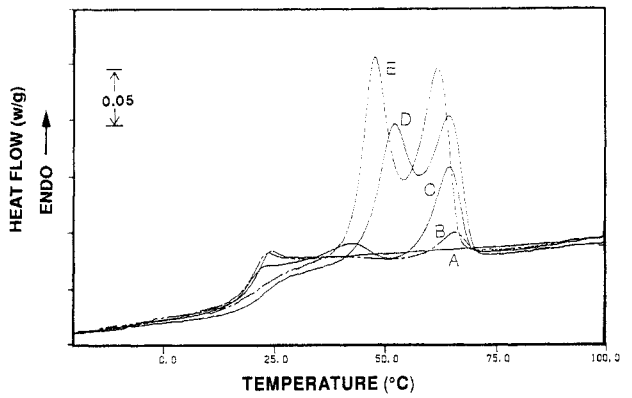

Figure 6. DSC traces for a polyurethane (M_n = 59K). Curves: (A) aging time at room temperature, t_a, <1 day; (B) t_a = 2 days; (C) t_a = 4 days; (D) t_a = 31 days; (E) t_a = 217 days.

used in place of M_v, the best-fit value for a would be 0.59, and if M_n was used, it would be 0.84. The results indicate that for this material M_w is a good approximation for M_v. For ideal situations where the distributions in different batches are identical, the value for a is independent of the type of average molecular weight used. It has been asserted that for those molecular weight distributions that are most likely occurring in polymeric systems M_v is close to M_w.[15] This approximation was affirmed with our materials.

Endothermic Behavior. The thermal properties of this polymer were studied by following the time evolution of the endothermic behavior of a high molecular weight sample (M_n = 59K) with DSC. In preliminary DSC scanning, the tail of the highest discernible transition was located at ~80 °C, and there was no exothermic peak observed during the quenching. Thus, heating a specimen to 100 °C in DSC for 5 min followed by quenching it to room temperature produced an amorphous specimen. Any observed change in endothermic behavior in subsequent DSC scanning was due to aging at room temperature.

DSC traces for this polyurethane are characterized by a set of multiple endothermic peaks which evolve with time. This attribute is illustrated in Figure 6; curves A–E were obtained using specimens aged at room temperature for 0, 2, 4, 31, and 217 days, respectively. An endothermic peak at about 66 °C occurred after 1 day of aging, the height of this peak increased with time, and the position shifted to lower temperatures. At 217 days, this peak was located at 62 °C. A second peak appeared at 42 °C after about 4 days. The height of the 42 °C peak also increased with time. The position initially moved to higher temperatures (52 °C after 31 days) and then shifted to lower temperatures, approaches 48 °C at 217 days. Peak

Table II
Endothermic Peaks and ΔH_f as Functions of Time for Polyurethane 2, M_n = 59K, Aged at Room Temperature

aging time (day)	peak 1		peak 2		heat of fusion (J/g)
	T_m (°C)	height (W/g)[a]	T_m (°C)	height (W/g)	
1			65.8	0.011	0.231
2			65.5	0.017	0.485
4	42.1	0.015	64.5	0.078	4.23
8	48.8	0.081	64.7	0.117	11.9
16	53.8	0.130	64.8	0.120	13.6
31	52.3	0.127	64.3	0.128	14.5
64	53.1	0.163	64.0	0.126	14.9
187	49.3	0.164	62.4	0.138	15.4
217	48.1	0.179	62.0	0.167	16.0

[a] Heating rate = 10 °C/min (to obtain values in J/°C·g, multiply the listed values by 6).

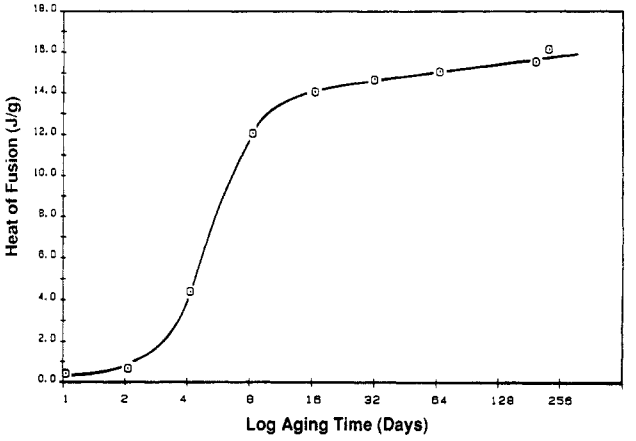

Figure 7. Heat of fusion for a polyurethane (M_n = 59K) as a function of time. The solid line is added to guide the eye.

positions, peak heights, and heats of fusion, all as functions of time, are compiled in Table II. The heat of fusion is plotted against the aging time in Figure 7. An inflection point can be found at about 3.7 days, coincident with the appearance of the second peak described above. The nature of the transitions represented by the endothermic peaks and the significance of the inflection point are not fully understood. Similar multiple endothermic behavior has been observed in the hard segments of several polyurethanes[17-20] and model urethane compounds.[21] The morphology of those hard segments has been investigated using optical and electron microscopy[22] as well as X-ray scattering analysis,[18,22,23] and several possible origins for the multiple endothermic behavior have been proposed. They are molecular weight segregation,[24] coexistence of crystalline and paracrystalline phases,[23] polymorphism,[18,22] and microphase-separation transition.[17] It is also possible that each of the segments of the material forms a separate ordered domain.[25] Because the morphology of **2** is unknown, it is not possible to differentiate among the many possible origins of the observed melting endotherms.

As shown in Figure 7, ΔH_f for this polymer levels off toward 16 J/g. By way of comparison, this value is far less than ΔH_f for poly(tetrafluoroethylene) (PTFE), 83 J/g,[26] but is comparable to that for a semicrystalline copolymer of tetrafluoroethylene and hexafluoropropylene (FEP), 24 J/g.[27]

Intermolecular hydrogen bonding between C=O and N–H has been studied in polyurethanes as a function of temperature by infrared spectroscopy.[28,29] A similar analysis has been performed on **2** to explore the underlying processes responsible for the observed ordering phenomena. The IR spectrum of a specimen was monitored as a function of time at room temperature. Spectra taken at less than 6 h, 2 days, and 45 days after the preparation of

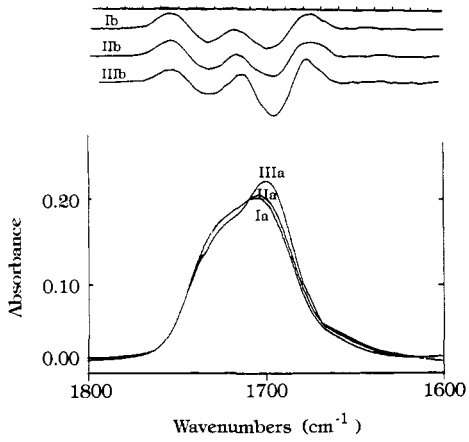

Figure 8. Infrared for polyurethane 2 (M_n = 33K) as a function of time. Upper "b" curves, second derivative of lower "a" spectra: (Ia and Ib) aging time less than 6 hours; (IIa, IIb) 2 days; (IIIa, IIIb) 45 days.

the film specimen by solvent casting as well as second-order derivative spectra are shown in Figure 8. In that figure the ordinate for the lower half is the absolute absorbance. As indicated by the DSC traces in Figure 6, the three time periods chosen represent three different morphologies. That is, the specimen at day zero shows no endothermic peak in the DSC trace, while at day two it shows one endothermic peak and at day 45 two.

Our analysis of these spectra focused on the 1800–1600-cm^{-1} (C=O stretching) range. With regard to analysis, application of "curve-fitting" techniques to the analysis of vibrational spectra has been discussed in an excellent review by Maddams.[30] The parameters to be found are the number of component bands, the positions of the band centers, the intensities, and the width of the bands. The degree of complexity involved in the determination of these parameters depends on "the separations of the component peaks in relation to their widths, and also of their relative intensities".[30]

A visual inspection of the spectra shown in Figure 8 reveals that each of the IR spectra is composed of two absorptions of about the same intensity and bandwidth. These peaks are separated from each other by about one and a half "half-bandwidths". For such component bands, good *estimates* for the value of the parameters can be obtained from absorption and second-derivative spectra without using repetitive calculations.

The shapes of the two components are assumed to be described by Gaussian functions; thus

$$\Gamma(n) = \Gamma_F(n) + \Gamma_{HB}(n) = \alpha_F \exp\{-0.5[(n - \bar{n}_F)/\sigma_F]^2\} + \alpha_{HB} \exp\{-0.5[(n - \bar{n}_{HB})/\sigma_{HB}]^2\} \quad (5)$$

where Γ = a function describing the IR spectrum, n = wavenumbers (cm^{-1}), Γ_F = a Gaussian function describing the free C=O stretching band, Γ_{HB} = a Gaussian function describing the hydrogen-bonded C=O stretching band, α = intensity of the component band, $\bar{n}$ = band center (cm^{-1}), and σ = standard deviation of the Gaussian function (cm^{-1}). The second derivative of Γ is

$$\Gamma''(n) = \Gamma_F(n)(1/\sigma_F)^2\{[(n - \bar{n}_F)/\sigma_F]^2 - 1\} + \Gamma_{HB}(n)(1/\sigma_{HB})^2\{[(n - \bar{n}_{HB})/\sigma_{HB}]^2 - 1\} \quad (6)$$

The band centers, $\bar{n}_F$ and $\bar{n}_{HB}$, can be determined from the second-derivative spectrum by locating the two local minima. The intensities can be determined from the IR spectrum: since $\Gamma_{HB}(\bar{n}_F) \approx 0$, by eq 5, $\Gamma(\bar{n}_F) \approx \alpha_F$, and, similarly, $\Gamma(\bar{n}_{HB}) \approx \alpha_{HB}$. Noticing that $\Gamma''(\bar{n}_F - \sigma_F) \approx 0$ and $\Gamma''(\bar{n}_{HB} + \sigma_{HB}) \approx 0$, one finds σ_F and σ_{HB} from the second-derivative spectrum.

Table III
Parameters for the Component Bands in 2

aging time (days)	$\bar{n}_F$ (cm^{-1})	α_F	σ_F (cm^{-1})	$\bar{n}_{HB}$ (cm^{-1})	α_{HB}	σ_{HB} (cm^{-1})
<1	1733.2	0.139	11.6	1699.0	0.178	12.2
2	1732.5	0.142	11.6	1698.0	0.185	12.0
45	1732.1	0.135	11.7	1697.1	0.204	11.7

Table IV
Fraction of Free C=O Groups as a Function of Time in 2

aging time (days)	$\alpha_F\sigma_F$	$\alpha_{HB}\sigma_{HB}$	% free C=O	
			k = 1.0	k = 1.7
<1	1.61	2.17	43	56
2	1.65	2.22	43	56
45	1.58	2.39	40	53

Using the methods described above, we have found the parameters for the component bands for the IR spectra. The values are listed in Table III. The area under a Gaussian curve, representing the concentration of the species, is proportional to the product of the intensity and the standard deviation, $\alpha\sigma$. Such values for the free and hydrogen-bonded C=O stretching bands for each of the IR spectra are shown in Table IV. From these values, the fraction of free C=O groups can be calculated from equation

$$\% \text{ C=O}_F = 100\alpha_F\sigma_F/(\alpha_F\sigma_F + \alpha_{HB}\sigma_{HB}/k) \quad (7)$$

In eq 7, k is the ratio of the absorptivity coefficients. This value usually is determined by statistical methods. Due to the small number of our data points, we bypassed this step and used the literature value. Senich and MacKnight[28] reported a value for k at 1.05; Coleman, Painter, and co-workers reported a value at 1.71.[29] Using k = 1.0, we found the % C=O$_F$ to be 43, 43, and 40, respectively, for the specimens aged less than 1 day, 2 days, and 45 days; using k = 1.7, the corresponding values are 56, 56, and 53, respectively.

The above analysis gives semiquantitative weight to what is apparent from visual examination of Figure 8: the free C=O to hydrogen-bonded C=O ratio decreases with time. Recalling that the thermal analysis data discussed previously show an increase in ordered domains with time, one concludes that increased intermolecular hydrogen bonding correlates with an increase in the ordered domains. This conclusion is similar to those from infrared thermal analysis reported in the literature on related systems.[28,29]

Mechanical Properties. In this work, "crystalline" is used to describe the ordered state which develops in 2. Due to the lack of X-ray or other scattering data, the structure of the ordered regions cannot be determined at present. Furthermore, considering the structure of the diol 1, which has a chiral center at the CF carbon, and the presence of 5% of a minor geometric isomer, the existence of a rigorously crystalline phase is unlikely. Nevertheless, the occurrence of the ordered state has significant effects on the mechanical properties as detailed in this section.

Dynamic mechanical properties of the polyurethane was evaluated using a Rheovibron dynamic viscoelastometer. In Figure 9, storage moduli for two polyurethanes of different molecular weights are shown as functions of temperature. Both curves exhibit behavior typical for polymers of a low degree of crystallinity. The glass transition signaled by the accompanying decrease in the storage modulus occurs at 15–30 °C for polymers of lower molecular weight and 25–40 °C for polymers of higher mo-

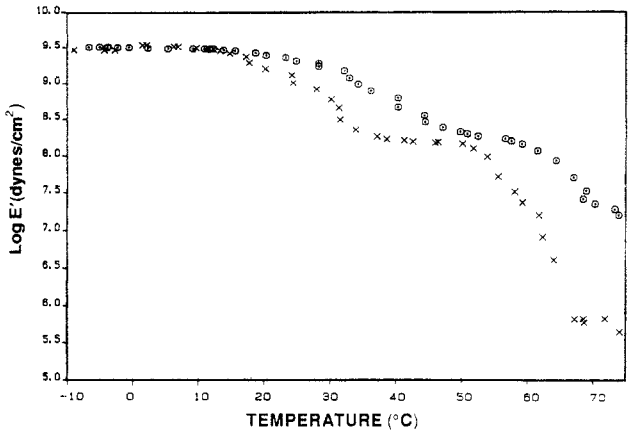

Figure 9. Storage moduli as functions of temperature for two polyurethanes of different molecular weights: (×) M_n = 33K; (⊙) M_n = 18K.

lecular weight. In the glassy state, the shape of the modulus curve is independent of the molecular weight, reflecting that short-range segmental motions are the determining factor.[31] On the other hand, at higher temperatures, translational motion of the whole molecule becomes dominant and the modulus is molecular weight dependent. Thus a steeper drop in the modulus is associated with a lower molecular weight.

Effects of molecular weight and crystallinity on mechanical properties were assessed. Samples of three different molecular weights each at two different levels of crystallinity were prepared for the stress–strain test. The two different degrees of crystallinity were achieved by allowing the samples to crystallize at room temperature for less than 6 h and 1 week, respectively. Small pieces were cut from each sample before and after the test. These pieces were examined with DSC to determine how the application of an external stress affects the crystallinity. Results from this combination of mechanical and calorimetric experiments are shown in Figure 10. Each frame in Figure 10 contains results for a different sample. DSC traces before and after the mechanical test are represented by the solid and broken curves, respectively; the stress–strain curve is shown as an inset. Heat of fusion values for these samples as functions of molecular weight, crystallization time, and external stress are summarized in Table V.

The initial rate and the extent of crystallization at a given time decrease with increasing molecular weight as shown in column 4 of Table V. Since a higher degree of crystallinity should result in a higher initial modulus, samples of the lowest molecular weight species showed the highest initial moduli (insets in Figure 10, frames Ia and Ib). Ductility of a material depends on both molecular weight and degree of crystallinity. The strain at break decreased with increasing crystallinity in samples of the two species of lower molecular weight (compare insets in Figure 10, frames Ia and Ib, IIa, and IIb). A decline in ductility was not observed in samples of the highest molecular weight. Insets in Figure 10, frames IIa and IIIa, show that the rigidity of the low crystalline samples of the two higher molecular weight species increases after the strain exceeding 400%. The degree of crystallinity was found to become higher at the end of the test for those two situations, and the increase in the rigidity was presumably due to the additional crystallization induced by the stretching of the samples. This stiffening phenomenon was not prominent when the samples were of moderate degrees of crystallinity (see insets in Figure 10, frames IIb and IIIb).

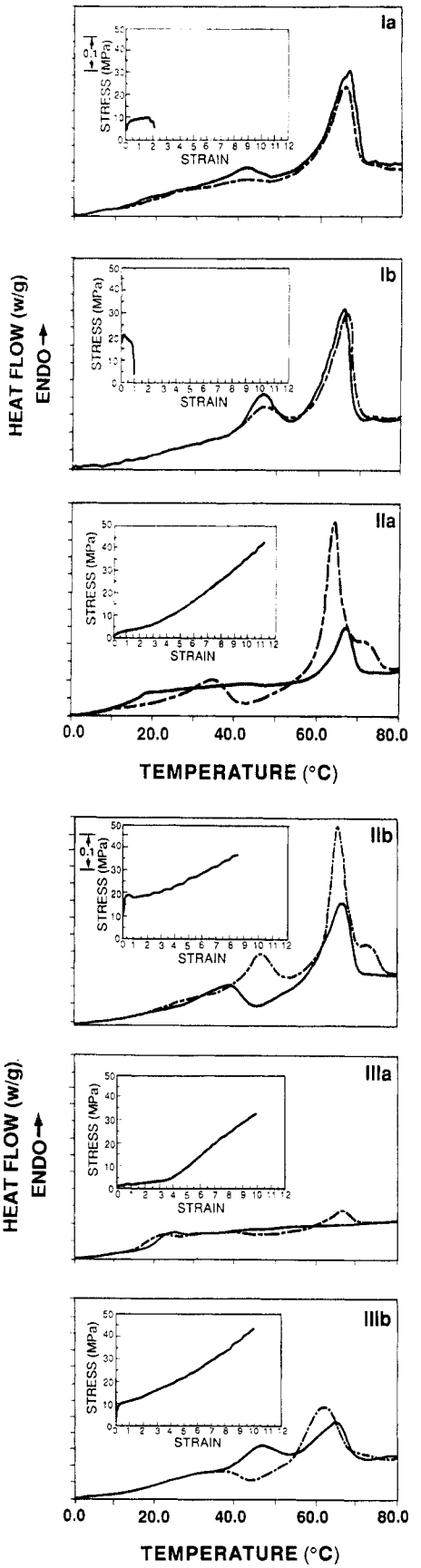

Figure 10. Stress–strain curves and DSC traces for polyurethanes. Solid curve, fresh film; broken curve, stretched film. Strain rate = 1.67 min^{-1}. Frames: (Ia) M_n = 18K, crystallization time, t_c, <6 h; (Ib) M_n = 18K, t_c = 145 h; (IIa) M_n = 39K, t_c < 6 h; (IIb) M_n = 39K, t_c = 145 h; (IIIa) M_n = 59K, t < 6 h; (IIIb) M_n = 59K, t_c = 145 h.

The DSC traces revealed that the application of an external stress changed the crystalline morphology of the polymer. This effect is molecular weight dependent. For

Table V
Heat of Fusion for the Polyurethane as a Function of Molecular Weight and Crystallization Time for 2

sample	MW[a]	crystallzn time, t_c	ΔH_f[b] (J/g) fresh	ΔH_f[b] (J/g) stretched[c]
Ia	18K	<6 h	14	12
Ib	18K	1 week	19	19
IIa	39K	<6 h	4.2	10
IIb	39K	1 week	15	14
IIIa	59K	<6 h	0	2.1
IIIb	59K	1 week	11	10

[a] M_n from GPC measurements. [b] ΔH_f for comparison: poly(tetrafluoroethylene), 82 J/g; poly(tetrafluoroethylene-*co*-hexafluoropropylene), 24 J/g; *n*-hexane, 152 J/g. [c] After a stress–strain test in an Instron tester.

samples of lowest molecular weight (M_n = 18K), stretching did not cause major changes in either the extent of crystallization or the positions of the melting peaks. In frames Ia and Ib, DSC traces for this type of polymer showed basically the same characteristics before and after the mechanical test.

In frame IIa, the sample (M_n = 39K, and room-temperature crystallization time, t_c, <6 h) originally had one melting peak at 67 °C with heat of fusion at 4.2 J/g. After the mechanical test, ΔH_f increased to 10 J/g. The mechanical test was completed in less than 1 h. This additional time is too short to account for any measurable fraction of increase in ΔH_f. Melting peaks were observed at 35 (minor) and 64 °C (major) as well as a shoulder at 72 °C, and recrystallization occurred at 42 °C. In frame IIb, the sample (M_n = 39K, t_c = 1 week) started with two melting peaks at 47 and 67 °C, respectively, and the total ΔH_f was 15 J/g. Stretching did not increase the degree of crystallinity (ΔH_f, 14 J/g), but rather it changed the crystalline morphology, as a minor melting peak was observed around 39 °C, a recrystallization peak at 46 °C, a major melting peak at 65 °C, and a shoulder at 73 °C.

In Figure 10, frame IIIa, the sample (M_n = 59K, t_c < 6 h) showed no trace of crystallinity before the stress–strain test but a single melting peak at 65 °C after it. This new peak indicates stress-induced ordering in the sample, although the extent of crystallization was low (ΔH_f, 2.1 J/g). In frame IIIb, the sample (M_n = 59K, t_c = 1 week) initially had two melting peaks at 47 and 65 °C, respectively, and the total ΔH_f was 11 J/g. As with polymers of intermediate molecular weight (frame IIb), stretching did not increase the degree of crystallinity (ΔH_f, 10 J/g). Morphological changes occurred, however, as reflected in the changes in the melting endotherms. Two melting peaks (at 37 and 62 °C) as well as an exothermic recrystallization peak (at 43 °C) appeared in place of the peaks present before stretching.

To summarize the results from the calorimetric measurements: (1) stretching induces ordering in amorphous and slightly crystalline polymers but not in moderately crystalline polymers with heats of fusion greater than 10 J/g; (2) stretching alters the crystalline morphology of the polymers, the effect being more noticeable in higher molecular weight polymers which are already moderately crystalline; and (3) stress induces recrystallization at high molecular weight polymers with moderate degrees of crystallinity.

Conclusions

Polyurethane **2** is a novel polymer with interesting time-dependent physical and mechanical properties. In this respect, **2** is unlike polymers derived from diols with multiple perfluoropropene addition (Scheme I; $x + y$ = ~2 or ~3). The synthesis and characterization of the latter polymers which are amorphous will be reported separately. Interestingly, despite the apparent crystallinity of **2** the polymer is optically clear even after aging at ambient temperature for more than 1 year. This observation indicates the ordered domains are smaller than the wavelength of visible light (ca. 400 nm). Although initially very tough, **2** becomes somewhat brittle after 1 year of aging at ambient temperature. We have initiated a solid-state NMR study to elucidate further the molecular basis of the aging phenomenon. In addition, a study of surface properties and bioadhesion of **2** and related polymers is underway.

Acknowledgment. This research was supported in part by the Office of Naval Research. The authors thank Drs. Kurt Baum and Aslam Malik of Fluorochem, Inc., for valuable discussions.

References and Notes

(1) This work was performed at Materials Chemistry Branch, U.S. Naval Research Laboratory. Correspondence should be addressed to: Code 6120, U.S. Naval Research Laboratory, Washington, DC 20375-5000.
(2) Evans, C. J. *Tin Its Uses* **1978**, *115*, 11.
(3) Phillip, A. T. *Prog. Org. Coat.* **1973**, *2*, 159.
(4) Atherton, D. *Org. Coat. Appl. Polym. Sci. Proc.* **1978**, *39*, 380.
(5) Atherton, D.; Verborgt, J.; Winkeler, M. A. M. *J. Coat. Technol.* **1979**, *51*, 88.
(6) Lewis, J. A. *Surf. Coat. Aust.* **1988**, 18–25.
(7) Brady, R. F.; Griffith, J. R.; Love, K. S.; Field, D. E. *J. Coat. Technol.* **1987**, *59*, 113.
(8) Takakura, T.; Kato, M.; Yamabe, M. *Makromol. Chem.* **1990**, *191*, 625.
(9) Tortelli, V.; Tonelli, C. *J. Fluorine Chem.* **1990**, *47*, 199. Baum, K., private communication.
(10) Hollander, J.; Trischler, F. D.; Harrison, E. S. *Polym. Prepr. (Am. Chem. Soc., Div. Polym. Chem.)* **1967**, *8*, 1149.
(11) *The Sadtler Guide to the NMR Spectra of Polymers*; Sadtler Research Laboratories, Inc.: Philadelphia, PA, 1973; p 223.
(12) Fluorinated diols were provided by Dr. Kurt Baum, Fluorochem Inc., Azusa, CA.
(13) Saunders, J. H.; Frisch, K. C. *Polyurethanes: Chemistry and Technology. I. Chemistry*; Interscience Publishers: New York, 1962; p 150.
(14) Wong, S. W.; Frisch, K. C. In *Advances in Urethane Science and Technology*; Frisch, K. C., Klempner, D., Eds.; Technomic: Westport, CT, 1981; Vol. 8, p 75.
(15) Flory, P. J. *Principle of Polymer Chemistry*; Cornell University Press: New York, 1953; p 313.
(16) Yau, W. W.; Kirkland, J. J.; Bly, D. D. *Modern Size-Exclusion Chromatography*; Wiley: New York, 1979; Chapter 10.
(17) Seymour, R. W.; Cooper, S. L. *Macromolecules* **1973**, *6*, 48.
(18) Blackwell, J.; Lee, C. D. *J. Polym. Sci., Polym. Phys. Ed.* **1984**, *22*, 759.
(19) Leung, L. M.; Koberstein, J. T. *Macromolecules* **1986**, *19*, 706.
(20) Yoon, S. C.; Sung, Y. K.; Ratner, B. D. *Macromolecules* **1990**, *23*, 4351.
(21) Qin, Zh. Y.; Macosko, C. W.; Wellinghoff, S. T. *Macromolecules* **1985**, *18*, 553.
(22) Briber, R. M.; Thomas, E. L. *J. Macromol. Sci., Phys.* **1983**, *B22* (4), 509.
(23) Koberstein, J. T.; Stein, R. S. *J. Polym. Sci., Polym. Phys. Ed.* **1983**, *21*, 1439.
(24) Hesketh, T. R.; van Bogart, J. W. C.; Cooper, S. L. *Polym. Eng. Sci.* **1980**, *20* (3), 190.
(25) The authors thank one of the reviewers for suggesting this possibility.
(26) Lau, S. F.; Suzuki, H.; Wunderlich, B. *J. Polym. Sci., Polym. Phys. Ed.* **1984**, *22*, 379.
(27) Starkweather, H. W., Jr.; Zoller, P.; Jones, G. A. *J. Polym. Sci., Polym. Phys. Ed.* **1984**, *22*, 1431.
(28) Senich, G. A.; MacKnight, W. J. *Macromolecules* **1980**, *13*, 106.
(29) Coleman, M. M.; Lee, K. H.; Skrovanek, D. J.; Painter, P. C. *Macromolecules* **1986**, *19*, 2149.
(30) Maddams, W. F. *Appl. Spectrosc.* **1980**, *34* (3), 245.
(31) Aklonis, J. J.; MacKnight, W. J. *Introduction to Polymer Viscoelasticity*, 2nd ed.; Wiley-Interscience: New York, 1983; Chapter 3A.